Materials & Design 130 (2017) 488–500

Contents lists available at ScienceDirect

Materials & Design

journal homepage: www.elsevier.com/locate/matdes

Through-thickness microstructure and mechanical properties of electron beam welded 20 mm thick AISI 316L austenitic stainless steel

M. Alali*, I. Todd, B.P. Wynne

Department of Materials Science and Engineering, Sir Robert Hadfield Building, The University of Sheffield, Mappin St., Sheffield S1 3JD, United Kingdom

ARTICLE INFO

Keywords:
Electron beam welding
Austenitic stainless steel
Fusion zone
Secondary dendrite arm spacing
Microharness
Digital image correlation

ABSTRACT

Through thickness microstructure and mechanical properties of defect-free electron beam welded 20 mm thick AISI 316L austenitic stainless steel are investigated as a function of beam power. The weld microstructure characterised by columnar and equiaxed dendritic ferrite in an austenite matrix. The dendritic structure was finer at the bottom of the weld zone. A microstructural boundary called "Parting" was seen along the weld centreline. Tensile tests, using digital image correlation technique, demonstrated that the highest strain concentrated in the FZ. The bottom section of the weld metal showed yield strength of about 14–52 MPa higher than the top section. The ultimate tensile strength in the bottom of the weld was also about 4% higher than the top. The final fracture was detected in the parting region. It was observed from the EBSD scan that the grains in the weld zone contained a weak orientation and showed high Schmid factor intensity with interception between some strong grains and soft grains at the weld centerline boundary. This explains the high weld ductility and the failure to happen in the parting region.

1. Introduction

Fabrication of thick section stainless steel structures and components by welding is a commonly used method in many industry sectors, such as the nuclear, petrochemical and oil industries. Currently the most prevalent thick section welding processes are those based on arc welding, e.g. submerged arc welding and hot-wire tungsten inert gas welding. These methods are relatively slow, require many passes, and produce significant distortion and/or residual stress, leading to poor productivity [1]. This has led to the emergence of high power density techniques of laser and electron beam welding that provide high speed, deep weld penetration, and low distortion, making them ideally suited to join thick sections, particularly when a high depth to width ratio (D/W) and narrow heat affected zone (HAZ) are required [2,3].

Laser beam welding (LBW) can be performed without the requirement of strict atmospheric control and the laser can be delivered though an optical cable, giving the technique significant flexibility. Welding thick sections, however, requires very powerful lasers or less powerful lasers combined with technologies such as narrow gap welding [1]. Electron beam (EBW) welding, on the other hand, requires a vacuum but has much greater energy density and consequently can produce single pass welds with significant depth penetration, making it ideally suited for thick section welding [4,5]. This combined with innovations such as reduced pressure electron beam welding, which can be undertaken with local pressure control and thus does not require the whole component to be within a vacuum chamber makes the EBW a very attractive fabrication technology for large thick section structure critical applications, particularly nuclear fission pressure vessels and nuclear fusion vacuum vessels [6–8]. There is, however, limited knowledge of how microstructure and mechanical properties may vary through the thickness following EBW, which is a significant knowledge gap that must be filled before the maximum potential of the technology is fulfilled.

In general, the microstructures in the fusion zone (FZ) of austenitic stainless steel welds contain a variety of austenite and ferrite structures, depending on solidification behaviour and subsequent solid-state transformations, which are controlled by composition and cooling rate [9,10]. For conventional welding process, e.g. Tungsten Inert Gas (TIG), at low welding heat inputs, i.e. high cooling rates, the weld solidification mode is either fully ferritic (F) or ferritic/austenitic (FA) mode with the δ-ferrite in the form of dendritic lathy δ-ferrite [11,12]. However, for higher heat inputs the δ-ferrite can have a vermicular morphology with a coarse dendritic structure [13,14]. Welding techniques with high power density, i.e. low heat input and fast welding speed, such as the EBW and LBW can produce similar microstructures but with a finer grain size, e.g. small dendrite spacing and consequently high joint strength compared to conventional welding processes [15]. However, these very high welding speed processes can potentially cause

* Corresponding author.
E-mail address: msjalali1@sheffield.ac.uk (M. Alali).

http://dx.doi.org/10.1016/j.matdes.2017.05.080
Received 13 January 2017; Received in revised form 4 May 2017; Accepted 25 May 2017
Available online 29 May 2017

Table 1
Chemical composition (wt%) of used AISI 316L.

Element	Cr	Ni	C	Si	Mn	Mo	N	P	Cu	Co	N	Fe
wt%	16.63	10.14	0.031	0.46	1.32	1.87	0.08	0.027	0.67	0.11	0.08	Remainder

some microstructure changes, such as altering the solidification mode or ferrite morphology, directly impacting on the mechanical properties of the weld [16]. For instance, a change in the solidification mode from primary ferrite to primary austenite in laser beam welded AISI 304L stainless steel is often cited as the main reason for the weld solidification cracking [17,18]. It is also worthy to note that a clear line of microstructure morphology separation, e.g. columnar to equiaxed, called parting can often been observed in the middle of the FZ of EB Welded AISI 316 L austenitic stainless steel, which is considered the weakest area of the weld [19–21].

In this study, the through thickness microstructure and mechanical properties of defect-free electron beam welded 20 mm thick AISI 316L austenitic stainless steel are investigated as a function of beam power. This is done with the aim of identifying key aspects of the as-welded microstructure or its variation through the weld that will define its design requirements and limitations.

2. Experimental procedure

The material used in this study was 20 mm thick AISI 316L austenitic stainless steel, chemical composition in Table 1, received in the as-rolled and mill annealed condition. Three sets of welding parameters were investigated, shown in Table 2, using a universal type K40 chamber electron beam machine, (Probeam, Germany). The working pressure of the electron beam machine chamber was approximately 10^{-5} mbar and the accelerating voltage was 60 KV (constant). To obtain the maximum amount of weld material for each welding condition, two welds were applied perpendicular to the rolling direction (RD) on 3 plates with dimensions of 60 × 150 mm, Fig. 1. The weld conditions were chosen based on bead on plate and butt joint trails to attain the optimum welding parameters in terms of full penetration and weld profile, with the aid of radiographic testing to ensure the weld was defect free. The edges of the plates were carefully machined by milling before performing the welds in order to obtain a perfect square butt joint and to ensure the gap between the two plates was as narrow as possible.

Material for microstructure analysis was prepared using standard grinding and polishing. To reveal the microstructure, the polished samples were etched in a mixture of equal amounts of HCL, Acetic and HNO_3 acids for 20–25 s. The metallographic examination was implemented using a group of techniques including optical light microscopy, scanning electron microscope (SEM), energy dispersive X-ray (EDX) and electron backscattered diffraction (EBSD). The optical light microscope was performed using a Nikon Eclipse LV150 microscope and SEM was carried out using a field emission gun (FEG) Inspect F in secondary imagining mode. For the EDX and EBSD analysis, FEG Phillips XL30s and FEI Sirion electron microscopy were used respectively. Line intercept method [22–24] was used to measure the secondary dendrite arm spacing (SDAS) in the FZ in regions near the top, middle and bottom of the weld. The measurement of each sample's SDAS was applied to several micrographs, an example of which is shown in Fig. 2.

Table 2
EBW parameters used in weld manufacture.

Weld number	Chamber pressure (mbar)	Accelerating voltage (KV)	Beam current (mA)	Speed (mm/s)	Focus offset (mA)	Figure	Weld length (mm)
1	10^{-5}	60	100	9	− 5	Line	150
2	10^{-5}	60	110	9	− 5	Line	150
3	10^{-5}	60	120	9	− 5	Line	150

Fig. 1. Welded plates using weld number 2 parameters.

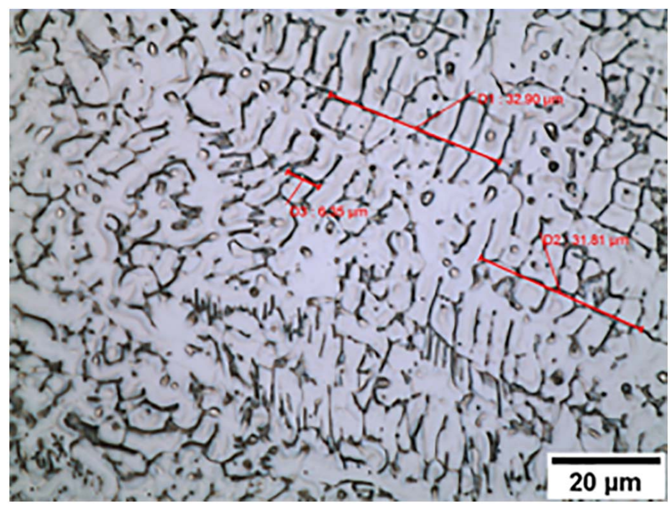

Fig. 2. Measurements of SDAS.

Mechanical property assessment of the welds was performed using microhardness and tensile tests. Vickers hardness measurements were taken in a two-dimensional grid with a 0.4 mm spacing covering the FZ, HAZ and part of the BM in the weld, as indicated in Fig. 3, using a 100 g load and 3 s dwell time. For the tensile test, three transverse tensile test specimens were extracted from each weld line and from the BM. The samples were cut from three locations across the thickness, (top, middle and bottom) and they were prepared according to ASTM E8M-04 guidelines [25], as shown in Fig. 4. The tensile tests were performed using a Zwick/Roll Z050 machine with a 50KN load cell and a cross-head speed of 0.1 mm/s at room temperature. To map the strain variation and characterize the mechanical behaviour of weld and heat affected zones during deformation, the Digital Image Correlation (DIC) technique was used during tensile testing. Before the test, the tensile samples were painted white, then with a random black speckle pattern to enable data capture by DIC. A high-resolution camera was used to take three pictures per second. The pictures were then analyzed using the vic-2D software to provide two-dimensional strain maps [26–28]. To map the deformation development inside the necking area with higher resolution and accuracy and to determine the weakest area in